Middle East Research Journal of Engineering and Technology
ISSN: 2789-7737 (Print) ISSN: 2958-2059 (Online)
Frequency: Bi-Monthly
DOI: https://doi.org/10.36348/merjet.2025.v05i01.002

KUWAIT SCHOLARS PUBLISHER
Website: http://www.kspublisher.com/
Email: office@kspublisher.com

Design of Half-wave Rectifier with Inductive Load for High Speed Converter Design in Charging Station of Electric Vehicles

Hnin Wint War Nyo[1*], Hla Myo Tun[2], Lei Lei Yin Win[1], Thanda Win[1], Mya Mya Aye[1], Khaing Thandar Soe[1], Devasis Pradhan[3]

[1]Department of Electronic Engineering, Yangon Technological University, Myanmar (Burma)
[2]Research Department, Yangon Technological University, Myanmar (Burma)
[3]ECE Department of Acharya Institute of Technology, Karnataka, India

Abstract: The paper presents the Design of Half-wave Rectifier with Inductive Load for High Speed Converter Design in Charging Station of Electric Vehicles. The research challenge in this study is to confirm the high speed converter design in charging station of electric vehicles. The mathematical modelling for AC to DC converter design is also evaluated. The SIMULINK model for AC to DC converter design is implemented. The simulation results from the implemented SIMULINK model were confirmed with the recent works. The designs are verified by MATLAB Simulink simulation tool. The results show that the efficiencies of converter with different rectifiers are above 92% at full load analyses.

Keywords: Half-wave Rectifier, Inductive Load, High Speed Converter, Electric Vehicles, Power Electronics.

Research Paper

***Corresponding Author:**
Hnin Wint War Nyo
Department of Electronic Engineering, Yangon Technological University, Myanmar (Burma)

How to cite this paper:
Hnin Wint War Nyo *et al* (2025). Design of Half-wave Rectifier with Inductive Load for High Speed Converter Design in Charging Station of Electric Vehicles. *Middle East Res J. Eng. Technol*, 5(1): 10-17.

Article History:
| Submit: 06.12.2024 |
| Accepted: 04.01.2025 |
| Published: 08.01.2025 |

A. INTRODUCTION

The global shift towards electric vehicles (EVs) is driven by the urgent need to reduce carbon emissions and mitigate climate change. At the core of EV technology is the battery system, which plays a pivotal role in determining vehicle performance, range, and safety [1-5].

An electric car or electric vehicle (EV) is an automobile that is propelled by one or more electric traction motors, using only energy stored in batteries. Compared to conventional internal combustion engine (ICE) vehicles, electric cars are quieter, more responsive, have superior energy conversion efficiency and no exhaust emissions and lower overall vehicle emissions [6-12].

Nowadays, researchers have focused on power converters for cost effective, limited space, efficiency and performance in some areas such as electric vehicle and data center. In electric vehicles, power converters are important in flowing electrical energy for storing battery, APM Power Module, motor and other components. The space is one of the important converter design considerations for EV. The switching frequency is increased to reduce converter size. As a result, switches losses become excessive and power in components is dissipated. The components become short life span and the size of cooling device such as fan will be large. Traditional PWM converters are operated in hard switching mode and cannot reduce switching losses. Therefore, overall efficiency will not become as expected design [12-16].

The paper is organized as follows. Section B presents the research method. Section C mentions the Effect of inductive load. Section D focuses on the Effect of freewheeling diode. Section E gives the SIMULINK model and analysis. Section F concludes the study.

B. RESEARCH METHOD

As only half the available power can be utilized, the circuit of Fig.1(a) is limited only to fractional horsepower machines. In the controlled half-wave circuit, the dc output voltage is controlled by varying the triggering angle (i.e. firing angle or delay angle α) at which the SCR (T) starts conduction.

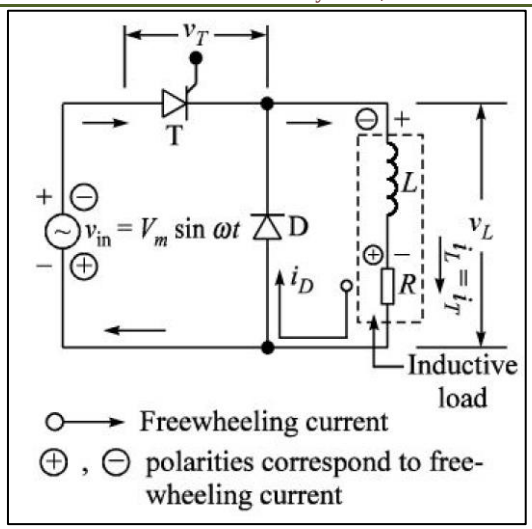

Figure 1: (a) Circuit diagram of a half-wave controlled rectifier for an inductive load

Let the SCR be triggered in the positive half-cycle at ωt = α. The SCR conducts and load current iL becomes the SCR current iT . The load current iL may continue to conduct beyond ωt = ϕ to a point decided by the time constant (T = L/R) of the inductive load. The SCR will turn off by natural commutation when the current iT becomes zero. By varying the firing angle α, load voltage vL can be changed. The power consumed by the load decreases as the triggering angle increases. The reactive power input from the supply increases with the increase in trigger delay α. The waveform of the load current in Fig.1(b) will be improved if the load be highly inductive, i.e. large time constant. The load current may even get prolonged up to the next conducting half-cycle to give continuous load current. The conduction angle β is dependent upon the time constant of the inductive load and firing angle α. The expression for the average output voltage (Vdc = VL) will be given by:

$$V_{dc} = \frac{1}{2\pi}\int_{\alpha}^{\alpha+\beta} V_m \sin\omega t \; d\omega t \quad (1)$$

Therefore,

$$V_{dc} = \frac{V_m}{2\pi}\left[\cos\alpha - \cos(\alpha+\beta)\right] \quad (2)$$

Current $i_L(t)$ in the circuit is given by

$$i_L(t) = \frac{V_m}{Z_L}\sin(\omega t + \alpha - \phi) + \left[\frac{V_m}{Z_L}\sin(\phi - \alpha)\right] e^{t/T} \text{ for } 0 \le t \le (\pi - \alpha)/\omega \quad (3)$$

where

V_m is the peak magnitude of the input voltage

Z_L is the load impedance

f is the power factor angle

T is the time constant of the inductive load.

During time period β, the current flows through the load downwards and the voltage across the load is negative from ϕ to (α + β).

The rms value of the load voltage will be given by

$$V_{load,rms} = \sqrt{\frac{1}{2\pi}\int_{\alpha}^{\alpha+\beta} V_m^2 \sin^2(\omega t)\, d(\omega t)} \quad (4)$$

Therefore,

$$V_{load,rms} = V_m \sqrt{\frac{1}{2\pi}\int_{\alpha}^{\alpha+\beta} \sin^2(\omega t)\, d(\omega t)}$$

$$V_{load,rms} = V_m \sqrt{\frac{1}{2\pi}\int_{\alpha}^{\alpha+\beta} \left[\frac{1-\cos 2(\omega t)}{2}\right] d(\omega t)}$$

$$V_{load,rms} = \frac{V_m}{2}\sqrt{\frac{1}{\pi}\int_{\alpha}^{\alpha+\beta} \left[1-\cos 2(\omega t)\right] d(\omega t)} \qquad (5)$$

$$V_{load,rms} = \frac{V_m}{2}\sqrt{\frac{1}{\pi}\left[(\omega t) - \frac{\sin 2(\omega t)}{2}\right]_{\alpha}^{\alpha+\beta}}$$

$$V_{load,rms} = \frac{V_m}{2}\sqrt{\frac{1}{\pi}\left[(\alpha+\beta-\alpha) - \frac{\sin 2(\alpha+\beta)}{2} + \frac{\sin(2\alpha)}{2}\right]}$$

$$V_{load,rms} = \frac{V_m}{2}\sqrt{\frac{1}{\pi}\left[\beta - \frac{1}{2}\{\sin 2(\alpha+\beta) + \sin(2\alpha)\}\right]}$$

The ripple factor is given by

$$\text{Ripple factor} = \frac{V_{load\ ripple(rms)}}{V_{dc}} = \frac{\sqrt{V_{load,\,rms}^2 - V_{dc}^2}}{V_{dc}} \qquad (6)$$

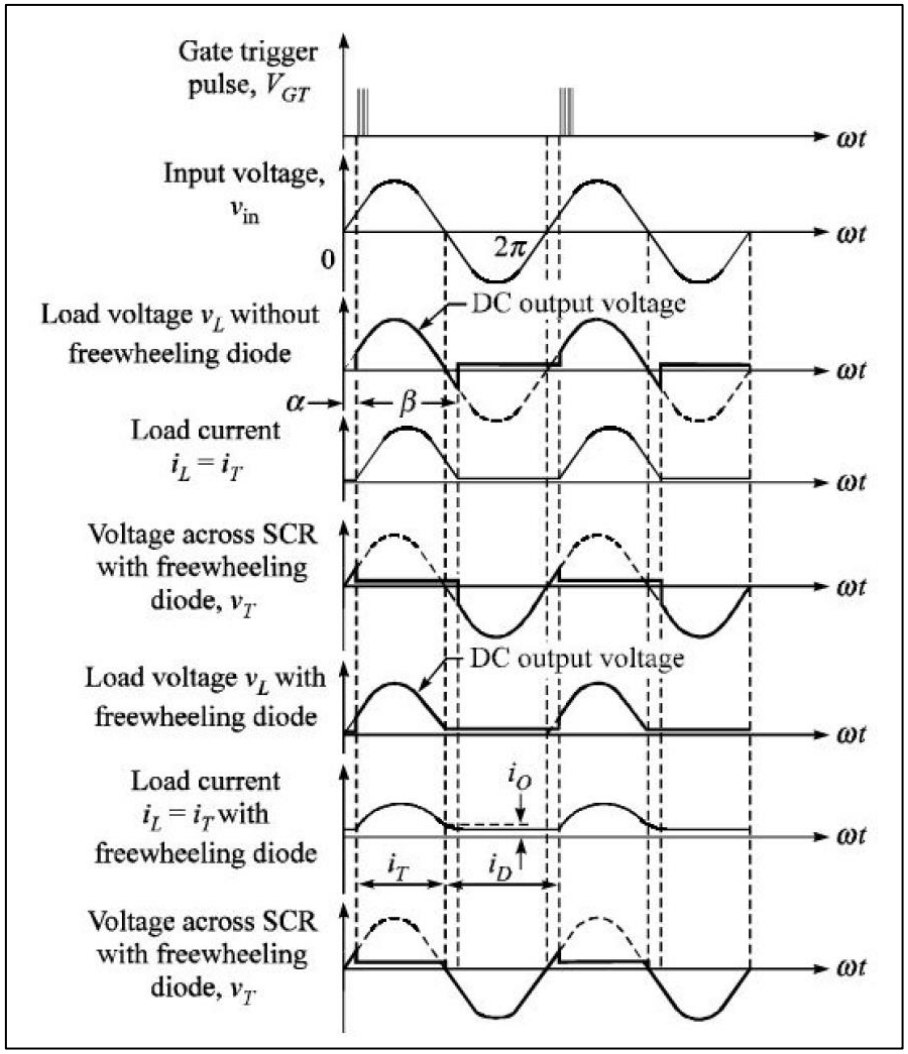

Figure 1: (b) Waveforms of a half-wave controlled rectifier for an inductive load

Therefore,

$$\text{Ripple factor}=\frac{\sqrt{\left[\frac{V_m}{2}\sqrt{\frac{1}{\pi}\left[\beta-\sin 2(\alpha+\beta)-\sin(2\alpha)\right]}\right]^2-\left[\frac{V_m}{2\pi}\left[\cos\alpha-\cos(\alpha+\beta)\right]\right]^2}}{\frac{V_m}{2\pi}\left[\cos\alpha-\cos(\alpha+\beta)\right]} \quad (7)$$

$$\text{Ripple factor}=\frac{\sqrt{\left[\frac{V_m^2}{2^2}\frac{1}{\pi}\left[\beta-\sin 2(\alpha+\beta)-\sin(2\alpha)\right]\right]-\frac{V_m^2}{2^2\pi^2}\left[\cos\alpha-\cos(\alpha+\beta)\right]^2}}{\left[\sqrt{\frac{V_m}{2\pi}\left[\cos\alpha-\cos(\alpha+\beta)\right]}\right]^2}$$

$$\text{Ripple factor}=\frac{\sqrt{\left[\frac{V_m^2}{2^2}\frac{1}{\pi}\left[\beta-\sin 2(\alpha+\beta)-\sin(2\alpha)\right]\right]-\frac{V_m^2}{2^2\pi^2}\left[\cos\alpha-\cos(\alpha+\beta)\right]^2}}{\sqrt{\left(\frac{V_m}{2\pi}\right)^2\left[\cos\alpha-\cos(\alpha+\beta)\right]^2}}$$

$$\text{Ripple factor}=\frac{\sqrt{\left[\frac{V_m^2}{2^2}\frac{1}{\pi}\left[\beta-\sin 2(\alpha+\beta)-\sin(2\alpha)\right]\right]-\frac{V_m^2}{2^2\pi^2}\left[\cos\alpha-\cos(\alpha+\beta)\right]^2}}{\sqrt{\frac{V_m^2}{2^2\pi^2}\left[\cos\alpha-\cos(\alpha+\beta)\right]^2}}$$

$$\text{Ripple factor}=\sqrt{\frac{\left[\frac{V_m^2}{2^2}\frac{1}{\pi}\left[\beta-\sin 2(\alpha+\beta)-\sin(2\alpha)\right]\right]-\frac{V_m^2}{2^2\pi^2}\left[\cos\alpha-\cos(\alpha+\beta)\right]^2}{\frac{V_m}{2\pi}\left[\cos\alpha-\cos(\alpha+\beta)\right]^2}}$$

$$\text{Ripple factor}=\sqrt{\frac{\left[\frac{V_m}{2\pi}\left[\beta-\sin 2(\alpha+\beta)-\sin(2\alpha)\right]\right]-\frac{V_m}{2\pi^2}\left[\cos\alpha-\cos(\alpha+\beta)\right]^2}{\frac{1}{\pi}\left[\cos\alpha-\cos(\alpha+\beta)\right]^2}} \quad (8)$$

C. Effect of inductive load

As the load consists of an inductance and a resistance, the waveform will be different from that obtained with a pure resistive load. In this case when the ac voltage passes through natural zero after ωt = ϕ, the SCR may not reach zero and may continue to conduct even when the voltage wave is passing through the negative half-cycle. According to Lenz's law, this is due to the fact that the current through the inductance cannot be suddenly reduced to zero. During the negative half-cycle of voltage, the current continues to flow till the energy is fed back to the source.

D. Effect of freewheeling diode

To overcome the problem of the inductive load, a freewheeling diode D is connected across the load. There are two modes of operations for this circuit. In the first mode, the SCR is triggered in the positive half-cycle at ωt = α, the diode D will be reverse biased and it fails to take any active part in the operation of the circuit from ωt = α to ωt = ϕ, when the SCR current iT will be the load current iL, i.e. this mode exists from the instant of triggering to the time when the supply polarity reverses. The current in this mode is given by

$$i_L(t)=\frac{V_m}{Z_L}\sin(\omega t+\alpha-\phi)+\left[\frac{V_m}{Z_L}\sin(\phi-\alpha)+i_0\right]e^{t/T}\ \text{for}\ 0\le t\le(\pi-\alpha)/\omega \quad (9)$$

where i0 is the load current when the SCR is triggered.

During mode 2, the diode D will reverse bias the SCR T and turn it off beyond ωt = ϕ. The load is thus isolated from the ac supply. The stored energy in the inductance of the load will find its path through diode D, thereby freewheeling current iD flows that decays exponentially. Hence the supply current lasts only for one half-cycle. If the load be sufficiently inductive, then the diode will maintain the load current up to the beginning of the next instant of triggering at ωt = 2ϕ+α as in Fig.1(b). During mode 2, the inductive energy of the load is dissipated in the load resistance R instead of returning to the input.

The conduction angle β is dependent upon the time constant of the inductive load and the firing angle α. By varying α, the load voltage vL can be changed. The

power consumed by the load decreases as the triggering angle α is increased. The current during this period is given by

$$i_L(t) = I_0 e^{-Rt/L} \text{ for } (\phi - \alpha)/\omega \le t \le 2\phi/\omega \quad (10)$$

The phase angle control of an inductive load in the presence of the freewheeling diode D will not only help to improve the waveform by making it continuous but also help to relieve the SCR from conducting load current with the reversing of the supply polarity. It is seen that for the same triggering angle α, the power consumption in the load will be more with a freewheeling diode. However, the power flow from the input takes place only during the conduction of SCR T. Therefore, the ratio of the reactive power flow from the input to the total consumed in the load is less for the phase angle control circuit with a free-wheeling diode D. In other words, the freewheeling diode improves the input power factor. This is because the inductive energy stored in the inductance L of the load, instead of going back to the input, dissipates in the load resistance R during the conduction period of the diode D. The expression for the average output voltage (Vdc =VL) with freewheeling diode will be given by

$$V_{dc} = \frac{1}{2\pi}\int_{\alpha}^{\pi} V_m \sin\omega t \; d\omega t \quad (11)$$

Therefore,

$$V_{dc} = \frac{V_m}{2\pi}\left[1 - \cos\alpha\right] \quad (12)$$

The rms value (effective value) of load voltage (with freewheeling diode) is

$$V_{load,rms} = V_{eff} = V_m\sqrt{\frac{1}{2\pi}\left[\int_{\alpha}^{\pi}\sin^2(\omega t)\,d(\omega t) + \int_{\pi}^{2\pi} 0\,d(\omega t)\right]}$$

$$V_{load,rms} = V_{eff} = V_m\sqrt{\frac{1}{2\pi}\int_{\alpha}^{\pi}\left[\frac{1-\cos 2(\omega t)}{2}\right]d(\omega t)}$$

$$V_{load,rms} = V_{eff} = V_m\sqrt{\frac{1}{4\pi}\int_{\alpha}^{\pi}\left[1-\cos 2(\omega t)\right]d(\omega t)}$$

$$V_{load,rms} = V_{eff} = V_m\sqrt{\frac{1}{4\pi}\left[(\omega t) - \frac{\sin 2(\omega t)}{2}\right]_{\alpha}^{\pi}}$$

$$V_{load,rms} = V_{eff} = V_m\sqrt{\frac{1}{4\pi}\left[(\pi-\alpha) - \frac{\sin 2(\pi)}{2} + \frac{\sin(2\alpha)}{2}\right]}$$

$$V_{load,rms} = V_{eff} = V_m\sqrt{\frac{1}{4\pi}\left[(\pi-\alpha) - 0 + \frac{\sin(2\alpha)}{2}\right]}$$

$$V_{load,rms} = V_{eff} = V_m\sqrt{\left[\frac{(\pi-\alpha)}{4\pi} + \frac{\sin(2\alpha)}{8\pi}\right]} \quad (10)$$

If α = 0, then the average output voltage is

$$V_{dc} = \frac{V_m}{2\pi}\left[1 + \cos\alpha\right]$$

$$V_{dc} = \frac{V_m}{2\pi}\left[1 + \cos 0\right] \quad (11)$$

$$V_{dc} = \frac{V_m}{2\pi}$$

and

$$V_{load,rms} = V_{eff} = V_m\sqrt{\left[\frac{(\pi-\alpha)}{4\pi}+\frac{\sin(2\alpha)}{8\pi}\right]}$$

$$V_{load,rms} = V_{eff} = V_m\sqrt{\left[\frac{(\pi-0)}{4\pi}+\frac{\sin(2\times 0)}{8\pi}\right]} \quad (12)$$

$$V_{load,rms} = V_{eff} = V_m\sqrt{\left[\frac{1}{4\pi}\right]}$$

$$V_{load,rms} = V_{eff} = \frac{V_m}{2}$$

The ripple factor is given by

$$\text{Ripple factor}=\frac{V_{load\ ripple(rms)}}{V_{dc}}=\frac{\sqrt{V_{load,\,rms}^2-V_{dc}^2}}{V_{dc}} \quad (13)$$

Therefore,

$$\text{Ripple factor}=\frac{\sqrt{\left[V_m\sqrt{\left[\frac{(\pi-\alpha)}{4\pi}+\frac{\sin(2\alpha)}{8\pi}\right]}\right]^2-\left[\frac{V_m}{2\pi}[1+\cos\alpha]\right]^2}}{\frac{V_m}{2\pi}[1+\cos\alpha]}$$

$$\text{Ripple factor}=\frac{\sqrt{\left[(V_m)^2\left[\frac{(\pi-\alpha)}{4\pi}+\frac{\sin(2\alpha)}{8\pi}\right]\right]-\left[\frac{(V_m)^2}{(2\pi)^2}[1+\cos\alpha]^2\right]}}{\frac{V_m}{2\pi}[1+\cos\alpha]}$$

$$\text{Ripple factor}=\sqrt{\frac{\left[(V_m)^2\left[\frac{(\pi-\alpha)}{4\pi}+\frac{\sin(2\alpha)}{8\pi}\right]\right]-\left[\frac{(V_m)^2}{(2\pi)^2}[1+\cos\alpha]^2\right]}{\left(\frac{V_m}{2\pi}\right)^2[1+\cos\alpha]^2}}$$

$$\text{Ripple factor}=\sqrt{\frac{\left[\frac{(V_m)^2}{4\pi^2}\left[\pi(\pi-\alpha)+\frac{\pi\sin(2\alpha)}{2}\right]\right]-\left[\frac{(V_m)^2}{(2\pi)^2}[1+\cos\alpha]^2\right]}{\left(\frac{V_m}{2\pi}\right)^2[1+\cos\alpha]^2}} \quad (14)$$

$$\text{Ripple factor}=\sqrt{\frac{\left[\left[\pi(\pi-\alpha)+\frac{\pi\sin(2\alpha)}{2}\right]\right]-\left[[1+\cos\alpha]^2\right]}{[1+\cos\alpha]^2}}$$

$$\text{Ripple factor}=\sqrt{\frac{(\pi^2-\pi\alpha)+\frac{\pi\sin(2\alpha)}{2}-[1+\cos\alpha]^2}{[1+\cos\alpha]^2}} \quad (15)$$

$$\text{Ripple factor}=\frac{\sqrt{(\pi^2-\pi\alpha)+\frac{\pi\sin(2\alpha)}{2}-[1+\cos\alpha]^2}}{[1+\cos\alpha]}$$

E. SIMULINK MODEL AND ANALYSIS

Figure 2 illsutrates the SIMULINK Model. Figure 3 shows the Simulation Results. The SIMULINK model was created based on the mathematical model of the developed system for Electric Vehicles' Applications. The performance of the developed system was confirmed based on the simulated waveforms from that SIMULINK model. The insights gained from these simulations are instrumental in advancing the field of electric vehicle technology and meeting the growing demands for sustainable and efficient transportation solutions. The robustness of the developed system confirm that the performance specification for the real-world applications.

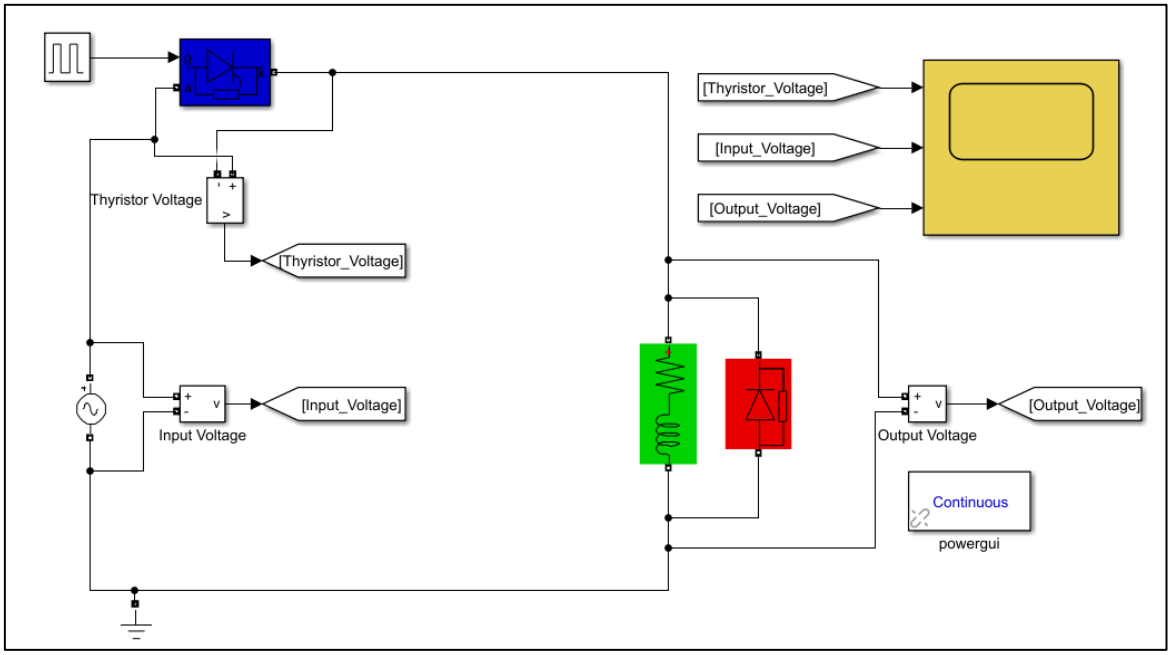

Figure 2: SIMULINK Model

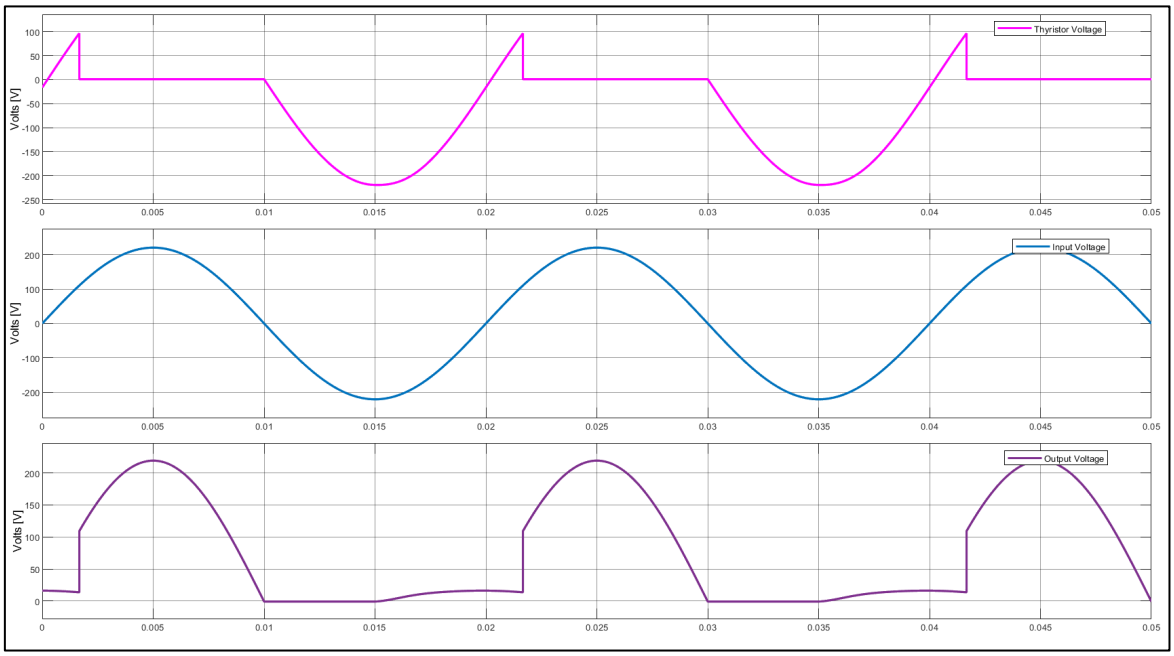

Figure 3: Simulation Results

F. CONCLUSION

The developed design of AC to DC converter for Electric Vehicles is very efficient and high performance condition for reality. The experimental studies were analyzed in the laboratory of YTU and the results confirm that the performance of the developed converter design met the targeted specification for research works. The robustness of the system was also

acceptable for real world applications. The performance accuracy could be enhanced with the updated technology like AI-driven smart converter design for future work.

G. ACKNOWLEDGMENT

The author would like to acknowledge many colleagues from the Electric Vehicle Engineering Research Group under the Department of Electronic Engineering of Yangon Technological University for providing the idea to complete this work.

REFERENCES

1. Htay, A. K., Tun, H. M. T., Pradhan, D., Win, L. L. Y., Khin, E. E., & Soe, K. T. (2024). Design of Multi-Level Inverter Design for Charging Stations of Electric Vehicles. *Andalasian International Journal of Applied Science, Engineering and Technology*, 4(2), 125-136. https://doi.org/10.25077/aijaset.v4i2.136.
2. Aung, M. M., Win, S., Thar, H. A., & Tun, H. M. (2024). Implementation of Efficient Electric Vehicle Fast Charging System Using Dual Active Bridge Converter. Andalasian International Journal of Applied Science, Engineering and Technology, 4(3), 278-287. https://doi.org/10.25077/aijaset.v4i3.172.
3. Lin, H., Aye, K. M., Tun, H. M., Theingi, & Naing, Z. M. (2008, October). Design and construction of intelligent traffic light control system using fuzzy logic. In AIP Conference Proceedings (Vol. 1052, No. 1, pp. 237-239). American Institute of Physics.
4. Octavia, N., Maung, M. M., & Tun, H. M. (2014). Performance Evaluation of Fuzzy Logic Controller in Water Bath Temperature Control System. International Journal of Science, Engineering and Technology Research, 3(6), 1623-1629.
5. Tun, H. M., & Aung, W. (2014). Analysis of Control System for A 24V PM Brushed DC Motor Fitted with an Encoder by Supplying H-Bridge Converter. Bahria University Journal of Information & Communication Technology, 7(1), 54.
6. Nwe, M. S., & Tun, H. M. (2017). Implementation of Multisensor Data Fusion Algorithm. International Journal of Sensors and Sensor Networks, 5(4), 48-53.
7. Hlain, N., Htun, Z., & Tun, H. (2015). Design and Implementation of PC Based over Speed Violation Management for Vehicles on Highway. International Journal of Scientific & Technology Research, 4(7), 74-77.
8. Oo, K. N., Naing, Z. M., & Tun, H. M. (2014). Implementation Of Distributed Control System in Process Control Management Using MATLAB. Int. J. Sci. Technol. Res, 3(6), 149-154.
9. Paing, S. M., Mon, S. S. Y., & Tun, H. M. (2016). Design And Analysis of Doppler Radar-Based Vehicle Speed Detection. IJSTR, 5(06).
10. Aung, N. P., Naing, Z. M., & Tun, H. M. (2016). Analysis of Time Delay Simulation in Networked Control System. International Journal of Electronics and Communication Engineering, 10(3), 359-364.
11. Khin, E. T., Myat, C., & Tun, H. M. (2015). Vehicles In Highway Communication System Using ZigBee and Bluetooth Network. Int. Jour. Sci. Tech. Res, 4(6), 425-429.
12. Thet, W. M., Maung, M., & Tun, H. M. (2015). Real-time vehicle data logging system using GPS and GSM. International Journal of Scientific and Technology Research, 4(07), 44-49.
13. Soe, T. T., & Tun, H. M. (2014). Implementation Of Double Closed-Loop Control System for Unmanned Ground Vehicles. international journal of scientific & technology research, 3.
14. Aye, P. P., & Tun, H. M. (2018). Analysis on Control System Design of Plant Simulator for Hardware-In-The-Loop Simulation Using MATLAB. International Journal of Sensors and Sensor Networks, 6(1), 1-7.
15. Lin, K. O., Tun, H. M., Naing, Z. M., & Moe, W. K. (2015). Microcontroller based SPWM single-phase inverter for wind power application. Int. J. Sci. Technol. Res., 4(8), 189-192.
16. Htay, Aung & Myo Tun, Hla & Lei, Lei & Khin, Ei & Pradhan, Devasis. (2024). Analysis of Step Up or Boost Converter Design for Charging Station of Electric Vehicles, IEMTRONICS 2024.